XXIV CONGRESS OF THE INTERNATIONAL SOCIETY OF BIOMECHANICS
XV BRAZILIAN CONGRESS OF BIOMECHANICS

EVALUATING THREE DIMENSIONAL HUMERAL SHAPE DEFORMATIONS IN CHILDREN WITH OBSTETRIC BRACHIAL PLEXUS PALSY

[1]Frances T. Sheehan, [1,2]Abrahm J. Behnam, [1,3]Katharine E. Alter and [1,4]Sylvain Brochard
[1]Rehab Medicine Department, National Institutes of Health, Bethesda, MD; [2]Virginia Commonwealth University School of Medicine; [3]Mt Washington Pediatric Hospital, Baltimore, MD; [4] Rehab Medicine Dept, University Hospital of Brest, France
email: fsheehan@cc.nih.gov, web: http://www.cc.nih.gov/rmd/fab/

INTRODUCTION

Obstetrical Brachial Plexus Palsy (OBPP) is a common birth injury, occurring in ~3 in every 1000 births [1]. Children who do not recover completely are left with shoulder muscle imbalance, contracture, and disuse leading to significant glenoid-humeral deformities. These deformities can severely limit the functional use of the arm and surgical intervention [2] is often recommended. Although glenoid retroversion and glenoid-humeral migration have been well studied, little is known about how OBPP affects the three-dimensional (3D) humeral morphology. Humeral external derotation osteotomies are often recommended and performed with knowledge limited to two-dimensional (2D) glenoid-humeral alignment [3]. This is in spite of the fact that restoring correct 3D morphology of the humerus is considered crucial for successful shoulder arthroplasty. In addition, pathological humeral head coronal plane rotation has also been shown to limit shoulder function [4], yet this deformation has not been studied in OBPP. One study that measured humeral version in children with BPP was limited to a 2D analysis [5].

The purpose of this study was to develop methodological techniques to measure the 3D humeral morphology in children with unilateral OBPP in order to test the following hypotheses: 1) The humeral head of the impaired arm demonstrates significantly different version than the unimpaired arm 2) The articular surface of the humeral head of the impaired arm is more inferiorly rotated, as compared to the unimpaired arm and 3) the humerii on the impaired side are smaller than on the unimpaired side. In addition, the 3D humeral morphological parameters were correlated with each other, as well as to subject specific characteristics.

METHODS

Sixteen children with unilateral OBPP were recruited for this IRB approved study. Each child provided written assent with a legal guardian providing written consent. Three children refused the MRI scan, leaving 13 subjects with an age range 6.7 to 18.8 years, five of whom had a left side involvement (4F/9M, age=11.8±3.3 years, height= 154.8± 21.4cm, weight=51.8±16.0kg, Mallet score = 15.1±3.0). Subjects were placed supine on the plinth of a 3T Siemens MRI (Verio, Germany) with the arm in as close to an

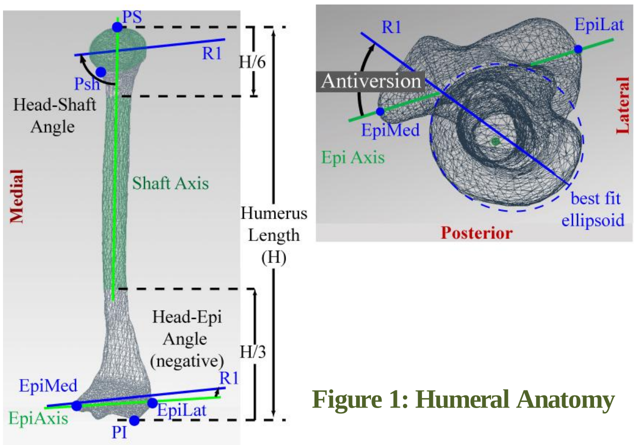

Figure 1: Humeral Anatomy

PS & PI: Most superior and inferior points. ***H*** = distance from PS to PD. ***EpiMed*** & ***EpiLat***: the most medial and lateral points, which creates the ***EpiAxis***. ***Psh***: point separating the head and shaft. ***R1–R3:*** the largest to smallest radius of the best fit ellipsoid to the humeral head. ***ShaftAxis***: the central axis of the best first cylinder to the humeral shaft. ***Version***: the acute axial plane angle between ***R1*** and ***EpiAxis*** (antiversion: the medial humeral head rotates anteriorly). ***Head-epi angle*** and ***Head-shaft angle***: the angles between ***R1*** and the ***EpiAxis*** and ***Shaft Axis***.

anatomically neutral position as possible and their palm facing the plinth (for comfort). Both the impaired and unimpaired arm were scanned, but were acquired independently, so that the shoulder could be positioned at isocenter. The order of scanning (impaired/unimpaired) was randomly assigned. A standard cardiac coil pair was wrapped anterior-posterior and lateral to the shoulder. If coverage was needed, a flex coil was wrapped around the elbow area. A T1-gradient recalled echo sequence was acquired, with all scanning parameters being held constant between subjects, except the field of view (416x312x192 pixels, slice thickness=1.2mm TR=16.6msec, TE=5.1msec, imaging time=5min 40sec). This resulted in a slight variation of resolution across subjects (0.55–0.63mm^2), enabling higher resolution for smaller subjects. When needed, a second scan was acquired in order to capture the distal humerus. Image data were stripped of identifiers and assigned a random number, blinding the researchers to the subject's identity and side of impairment.

A methodology was established and then applied to quantify 3D humeral morphology. The humeral head and elbow were segmented by manually outlining the cortical bone in every slice, whereas the shaft was segment using every 5th slice using MIPAV (Medical Image Processing, Analysis and Visualization, NIH, Bethesda, MD). The resulting VOI (volume of interest) was imported into Geomagic (Research Triangle Park, NC). Then a 3D mesh was fit to the points and smoothed using an upper deviation limit equal to one half the pixel size. Next, this model was aligned to its principle axes and its origin moved to the global origin. The separation between the shaft and head (***Psh***, Figure 1) was defined as the inflection point of the medial head curvature as it joins with the shaft. In addition, the most lateral and medial points of the epicondylar line were quantified (***EpiLat, EpiMed***). The model was then converted back into a point cloud. This point cloud, along with ***Psh***, ***EpiLat***, and ***EpiMed***, was imported into a customized Matlab program, which was used to determine: 1) the 3 radii of the best fit ellipsoid of the humeral head; 2) the central shaft of the best fit cylinder to the portion humeral shaft 33% from ***PI*** (most distal humeral point) and 17% from ***PS*** (most inferior humeral point), 4) the epicondylar width; 5) the humeral length (***H***); 6) the angle of the head relative to both the shaft and the epicondylar line (***Head-shaft*** and ***Head-epi angle***); and 7) humeral version. A paired Student's t-test was used to identify significant ($p<0.05$) differences between sides.

RESULTS AND DISCUSSION

The humeral head was elliptical and not spherical with the primary radius (***R1***) directed medially and the tertiary radius (***R3***) directed superiorly. In all measures of size (***R1***, ***R2***, ***R3***, and ***H***) the impaired side was smaller than the unimpaired (Table 1, $p<0.001$). The osseous atrophy was not uniform, with the superior-inferior dimension of the humeral head being affected the most. Specifically, the ratios of ***R1*** and ***R2*** to ***R3*** were both significantly larger on the impaired side, whereas ***R1/R2*** was no different (Table 1).

The ***Head-epi*** and ***Head-Shaft angles*** were no different between sides. This lack of significant difference was due to one subject who demonstrated a 26.6° increase in the ***Head-epi angle*** (> 2SD away for from the impaired average). When the one subject was removed there was a significant decrease in the ***Head-epi*** and ***Head-Shaft angle*** (Table 1: -8.8°, p=0.008 and -4.5°, p=0.04)**.** This novel finding is likely to become crucial in the management of OBPP because when such a deformity was created in cadavers, significant supraspinatus efficiency decreases and significantly higher arm elevation forces were seen [4]. Thus, neurological deficits resulting from the birth injury lead to muscle atrophy/contractures, which leads to boney deformations and these boney deformations appear to circle back and further weaken the shoulder complex.

The humeral head was anteverted on the impaired side (external rotation implying that the medial humeral head rotated anteriorly), and was retroverted on the control side. This matched well with previously documented 2D version in children with OBPP [5] and demonstrates an osseous compensation for the typical internally rotated arm posture seen in OBPP. Specifically, the humeral head external rotation partially compensates for the internal rotation of the arm and may help maintain glenoid-humeral congruency.

All size measures correlated with age (r = 0.68-0.76, $p<0.004$) for both sides. The ratio of ***R1*** and ***R2*** correlated with the ***Head-epi*** angle (r=0.62 and 0.68, $p<0.022$) on the control side only. The two head angles were correlated with each other (control: r=0.58, p=0.038 and impaired: r= 0.85, $p<0.001$). The unexplained variance between the ***Head-epi*** and the ***Head-shaft*** angles is due to the fact that the osseous deformations are not limited to the humeral head, but continue to the elbow as well. Age was inversely correlated with anteversion, but this was only significant on the impaired side (control: r=0.40, p=0.17 and impaired: r= 0.85, p=0.048). This was in agreement with the reported rapid change in humeral version in young children, with more moderate changes occurring up and through 16-19 years of age, when the version angle reaches adult levels [6].

CONCLUSIONS

This study is the first to evaluate 3D humeral shape changes in OBPP. In doing so, it demonstrates osseous atrophy in all three dimensions along with morphological changes resulting in the medial surface of the humeral head being rotated anteriorly and inferiorly. It was objectively shown that the entire humerus was affected. The documented 3D humeral shape changes are likely related to the well reported glenoid-humeral migration, glenoid version, internal rotation of the arm posture at rest, and limited external rotation range of motion. As the results did vary across subjects, we would recommend that a full, 3D, subject-specific glenoid-humeral shape analysis be carried out as part of any humeral or glenoid-humeral surgeries.

REFERENCES

1.Poyhia, T.H., et al.,*Radiology*, **254**. 253-60, 2010.
2.Abzug, J.M., et al.,*J Pediatr Orthop*, **30**. 469-74, 2010.
3.Poyhia, T., et al.,*Acta Orthop*, **82**. 482-8, 2011.
4.Voigt, C., et al.,*J Orthop Trauma*, **25**. 399-405, 2011.
5.van der Sluijs, J.A., et al.,*JBJSg Br*, **84**. 583-7, 2002.
6.Edelson, G.,*J Shoulder Elbow Surg*, **9**. 316-8, 2000.

Table 1: Paired differences in 3D humeral anatomy: ** indicates $p<0.001$

	R1	R2	R 3	R1/R2	R2/R3	R1/R3	H	Head-Epi	Version	Head- Shaft
BPP ave	20.8	17.7	15.2	1.18	1.18	1.38	269.8	1.9	-2.7	92.9
Control ave	21.5	18.2	16.6	1.19	1.09	1.30	288.0	9.4	14.5	95.0
Ave diff	**-0.7**	**-0.5**	**-1.5**	**-0.01**	**0.08**	**0.09**	**-18.2**	**-7.6**	**-17.2**	**-2.3**
p	**	**	**	0.886	0.017	0.044	**	0.092	0.023	0.436